Jenkins, J., Nobbs, A., Verkade, P., & Su, B. (2018). Characterisation of bactericidal titanium surfaces using electron microscopy. *Microscopy and Analysis (EMEA issue)*, *34*(1 (EU)), 17-22. http://www.microscopyebooks.com/Europe/2018/January/

Characterisation of bactericidal titanium surfaces using electron microscopy

Joshua Jenkins[1], Angela H. Nobbs[1], Paul Verkade[2], Bo Su[1]

[1] Bristol Dental School, University of Bristol, Bristol, BS1 2LY

[2] School of Biochemistry and Wolfson Bioimaging Facility, University of Bristol, Bristol, BS8 1TD

Tag line - Bactericidal TiO_2 nanostructures

Abstract

With the number of surgical procedures involving titanium implants rising annually, the total number of patients that develop bacterial infections also increases. Prevention of such infections has become of key importance for ensuring a patient`s wellbeing and to reduce hospital costs. As antimicrobial resistance emerges as a global healthcare threat, we sought to tackle this issue via an alternative, non-drug based approach. Here we describe a novel, nanostructured titanium surface capable of killing bacteria in a physical, contact-dependent manner. Using Electron Microscopy (EM) methods we demonstrate that titanium nanostructures stretch bacterial cells upon contact, leading to envelope rupture and cell deformation.

Introduction

In recent decades, the use of medical devices, including catheters, prosthetic heart values and orthopaedic implants, has increased substantially. This expansion has been driven by rising hospital admissions and the increased frequency of routine surgical procedures. Today, medical devices play an essential role in the management and treatment of patients, particularly those in intensive care [1–3]. Although technological advances continue to improve the performance and longevity of medical devices, all are susceptible to bacterial colonisation, which can lead to device failure and the onset of infection. Currently, medical devices are implicated in up to 70% of healthcare associated infections, corresponding to approximately 1.4 million infections in the U.S. annually [4].

Titanium medical implants, including replacement hip and knee joints, are prone to microbial colonisation during surgery. Upon attachment to the surface, bacteria can replicate to form dense aggregates embedded within an extracellular matrix, known as biofilms [4]. Once a biofilm has established, patients can develop prosthetic joint infections (PJIs). Treating PJIs is notoriously difficult due to the effects of immune depression in local tissues and the high degree of tolerance biofilms have against antibiotic therapies [5]. As a result, surgical revision is required to resolve most PJIs. However, these invasive and complex operations lead to prolonged hospitalisation for patients and significant treatment costs for healthcare providers, which can extend to £75,000 - £100,000 per patient [6].

Considering the increasing number of patients being referred to orthopaedic care annually, and the significant financial burden that PJIs pose to healthcare systems worldwide, substantial efforts are focused on developing alternative strategies to prevent biofilm formation on titanium implants [7]. With growing concerns over antibiotic resistance, a strong emphasis has been placed on approaches that work via physical, rather than chemical modes of action [8]. An area of growing interest is the field of biomimetics, where inspiration from nature is applied to the design and fabrication of surfaces with antibacterial properties.

Many natural surfaces have evolved strategies for reducing or preventing the accumulation of bacteria, including shark skin, the lotus flower and rice leaf [8] . The bactericidal properties of insect wings, including the cicada and dragonfly, have been widely reported [9–11]. These surfaces consist of nanostructure arrays that are believed to induce bacterial cell death through a process known as contact killing. The inspiration obtained from nature has led to the concept of biomimetic surfaces, where nanofabrication methods are used to recreate similar nanostructures on clinically relevant materials.

Aims

The bactericidal activity of natural and bioinspired surfaces is widely reported; however, the precise mechanistic basis for these effects remains elusive. This fundamental question must be answered if we are to improve the killing efficiency of nanostructured clinical materials. For contact killing to occur, bacteria must physically interact with the surface, therefore visualising this interface is crucial to progress our understanding of the mechanism causing cell death. To this end, electron microscopy techniques were developed to enable visualisation of the bacteria – nanostructure interface and improve our mechanistic understanding of contact killing.

Materials and Methods

Thermal oxidation

Square discs (8mm x 8mm x 1mm) were cut from a titanium alloy sheet (Ti-6Al-4V) and machine polished using silicon carbide paper. Polished discs underwent ultrasonic treatment in dH_2O at 40°C for 15 minutes. Clean samples were sealed inside a horizontal tube furnace. Prior to thermal oxidation, the furnace was purged with inert argon gas for a duration of 30 minutes. Following purging, a heating programme was initiated, raising the internal temperature of the furnace by 15°C/minute until a pre-defined maximum was reached. Once the final temperature was reached, vaporised acetone was transported into the tube to react with Ti-6Al-4V.

Bacterial strains and culture conditions

Staphylococcus aureus strain Newman, *Escherichia coli* strain K12 and *Klebsiella pneumoniae* (clinical isolate; kindly provided by M. Avison) were used in this study. Bacterial cultures were grown for 16 hours in Mueller-Hinton broth at 37°C, before being sub-cultured into fresh, pre-warmed medium and grown to early exponential phase. Titanium samples were sterilised in absolute ethanol, washed in dH_2O and dried prior to inoculation with bacterial suspensions (10^5 cells per disc). For imaging analysis, all surface types were incubated statically at 37°C for 3 hours.

Imaging analysis

A Quanta 200 FEI scanning electron microscope (SEM) was used to characterise the topography of surfaces generated by thermal oxidation and study the morphology of bacterial cells incubated on test surfaces. Bacteria were fixed in 2.5% glutaraldehyde (GA) in 0.1 M sodium cacodylate buffer for 1 hour on ice. Samples were then washed 3 x 5 minutes in buffer kept at 4°C. Following fixation, samples were dehydrated in a graded ethanol series of 25%, 50%, 70%, 90% and 100% for 10 minutes each. Samples where then critically point dried before sputter coating with gold and palladium.

A Tecnai 12 FEI 120kV BioTwin Spirit transmission electron microscope (TEM) was used to investigate the ultrastructure of bacterial cells incubated on test surfaces. Samples were fixed and washed as per SEM preparation. Post fixation was in 1% osmium (OsO_4) for 20 minutes. Samples were then washed before immersion in 3% uranyl acetate for 20 minutes. Samples were dehydrated as per SEM preparation and then soaked in epon resin for 90 minutes. Samples were placed at 60°C for 48 hours to allow resin polymerisation. Samples were then sectioned using a Leica EM UC6 ultramicrotome. TEM samples were stained post sectioning with uranyl acetate and lead citrate. A FEI Strata FIB201 was used to selectively mill Ti-6Al-4V test surfaces using a focused beam of gallium ions.

Results and Discussion

Characterising bioinspired nanostructures on titanium alloy

Randomly oriented titanium dioxide (TiO_2) nanostructures were grown on titanium alloy substrates via thermal oxidation. The processing conditions, including oxidation temperature and duration were changed in different batches. This led to the fabrication of two distinct nanostructured surfaces, referred to in this study as T1 and T2 (Figure 1A-B, D-E). Surface T1 comprised of nanostructures approximately 500 nm in length, with tip diameters between 30 - 50 nm and densities of 25 - 60 per μm^2. Surface T2 comprised of longer, less densely packed nanostructures, approximately 1 µm in length, with tip diameters between 30 - 150 nm and densities of 15 - 30 per μm^2. Elemental analysis was performed using energy dispersive x-ray spectroscopy (EDX) inside a TEM. The presence of titanium and oxygen were detected by point analysis, indicating that nanostructures were comprised of TiO_2 (Figure 1C, F).

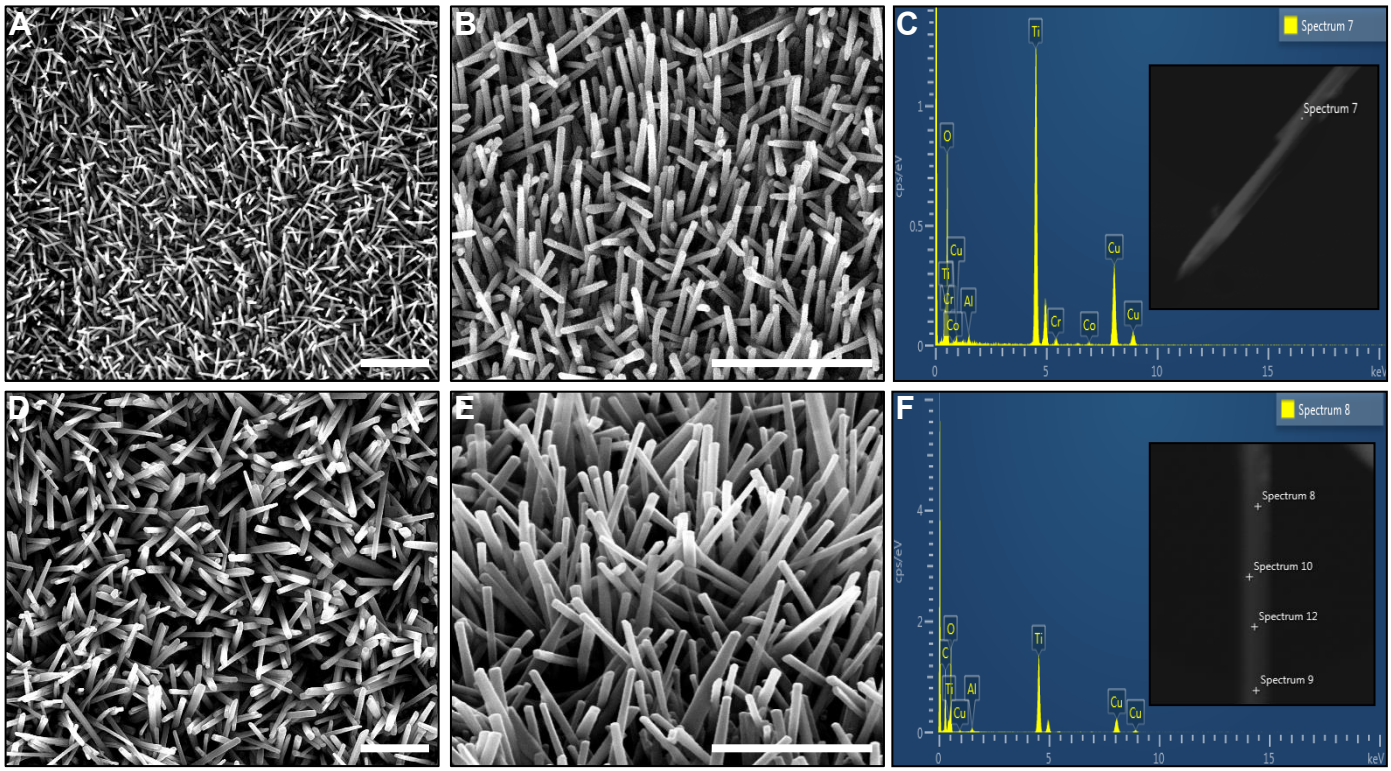

Figure 1. *SEM images of TiO_2 nanostructures generated on titanium alloy (Ti-6Al-4V) by thermal oxidation. Nanostructured surface T1 was generated at 715°C for 1 h (A-B). Nanostructured surface T2 was generated at 850°C for 5 minutes (D-E). EDX point analysis was performed under dark-field TEM, and the presence of titanium and oxygen was detected from both surfaces, indicating the presence of titanium dioxide. The detection of copper, chromium and cobalt were background signals (C, F). Scale bars 1 µm.*

Cross sectional analysis of titanium substrates by focussed ion beam scanning electron microscopy (FIB-SEM) revealed an oxide layer. The oxide layer is believed to act as a nucleation point from which the nanostructures grow (Figure 2A – D).

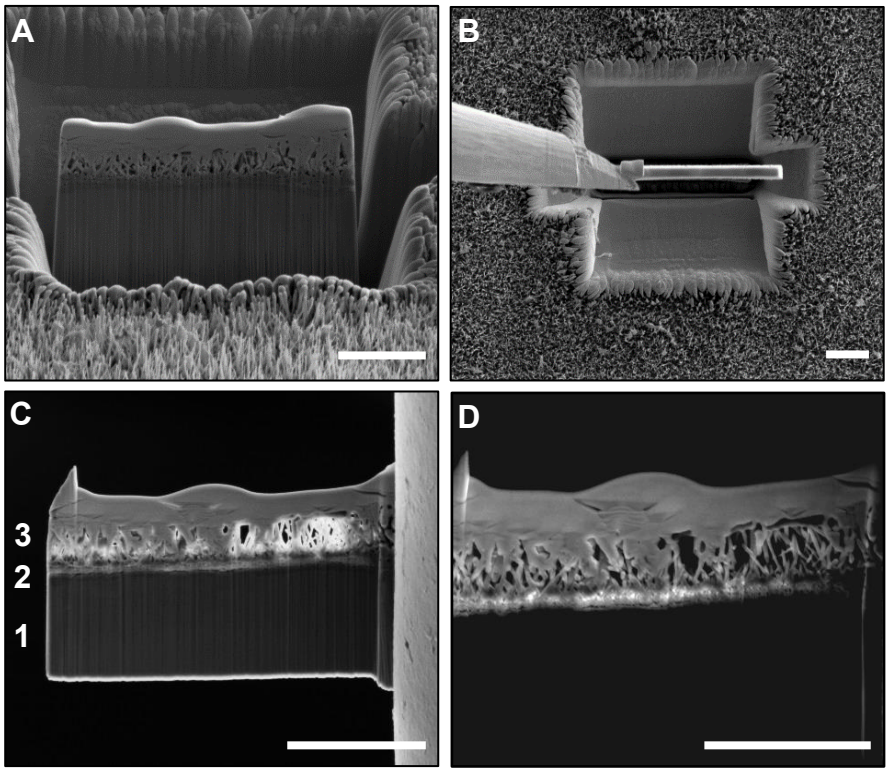

Figure 2. *FIB-SEM analysis of a nanopatterned titanium alloy substrate. A titanium alloy substrate comprised of TiO_2 nanostructures was milled by a gallium ion beam to generate a cross section (A). The section was attached to a nanomanipulator (B) and transferred to a FIB lift-out grid. The section was attached via platinum deposition. The section comprises of three distinct layers: 1) bulk titanium substrate, 2) nucleation layer, 3) titanium dioxide nanostructures (C-D). Scale bar 5 µm.*

Visualising bacteria - nanostructure interactions

SEM analysis

Scanning electron micrographs of *S. aureus*, *E. coli* and *K. pneumoniae* were taken on nanostructured surfaces T1 and T2; a flat titanium surface was used as a control. To visualise the cell - material interface, the microscope stage was tilted by 75°. On flat titanium surfaces, *S. aureus* cells displayed a characteristic coccoid (spherical) morphology, approximately 1 µm in diameter. *E. coli* and *K. pneumoniae* cells exhibited a bacillus (rod-shaped) morphology with a length of approximately 2 µm (Figure 3A.1 – C.1). The morphology of each bacterium on flat titanium surfaces was in keeping with that of healthy, viable cells. Furthermore, after 3 hours of static incubation, each bacterial species had formed microcolonies, an intermediate stage of biofilm formation [3]. On nanostructured surfaces T1 and T2, *S. aureus* cells displayed identical morphology to those on flat titanium surfaces, implying that cell structure was not significantly affected by the nanostructures (Figure 3A.2 - A.3).

In contrast, *E. coli* and *K. pneumoniae* cells showed distorted morphologies upon interacting with TiO_2 nanostructures on surfaces T1 or T2 (Figure 3B.2 – 3C.3). This effect was most pronounced on surface T2, where a single *E. coli* cell was pierced by multiple TiO_2 nanostructures. A nanostructure tip had pushed through one side of the cell and could be seen pressed against the opposite side; this interaction is most likely responsible for the marked reduction in cell thickness. These observations suggested that nanostructures can apply sufficient force across the envelope to rupture the cell, resulting in loss of turgor pressure and a collapsed morphology (Figure 3B.3). Similar morphologies were observed in *K. pneumoniae.* On both surfaces T1 and T2, the side of the cell in contact with nanostructures conformed to a concave shape, indicating the envelope was under stress.

The deformed morphologies observed in *E. coli* and *K. pneumoniae* compared to *S. aureus* are likely to reflect fundamental differences in cell envelope architecture. All bacteria possess a cell wall, composed of a repeating polymer chain called peptidoglycan that surrounds the cell. A key function of the cell wall is to provide structural support. In Gram-positive bacteria such as *S. aureus,* a thick peptidoglycan layer of between 20-80 nm lies external to the cytoplasmic membrane. In contrast, *E. coli* and *K. pneumoniae* are classified as Gram-negative bacteria, with a cell envelope comprising a much thinner peptidoglycan layer of typically 5-10 nm located between two plasma membranes. This key difference in cell envelope organisation may

explain why the structural integrity of *S. aureus* was not affected by the nanotopography, whilst *E. coli* and *K. pneumoniae* were affected [12].

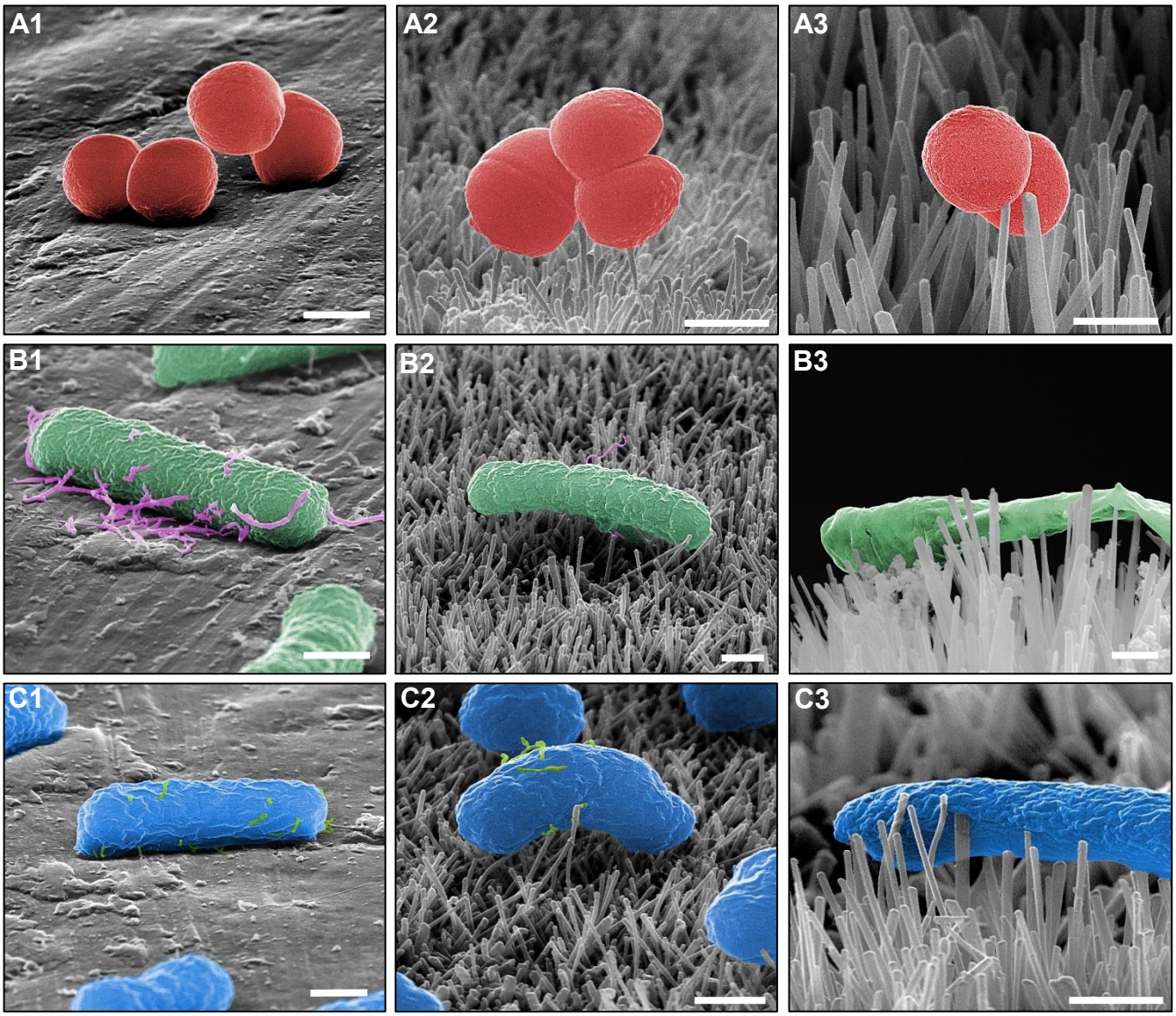

Figure 3. *False colour SEM images of S. aureus, E. coli and K. pneumoniae incubated on a control surface (A1, B1, C1), nanostructured surface T1 (A2, B2, C2) or nanostructured surface T2 (A3, B3, C3). The morphology of S. aureus did not change between surface types. In contrast, both E. coli and K. pneumoniae displayed abnormal morphologies on surfaces T1 and T2 and, in some cases, the cell structure had collapsed due to nanostructure piercing. Scale bar 500 nm, stage tilt 75°.*

TEM and FIB-SEM analysis

To investigate further if the deformation observed in *E. coli* and *K. pneumoniae* when in contact with TiO_2 nanostructures indicated that the cell envelope was structurally compromised, the ultrastructure of *K. pneumoniae* was analysed using TEM and FIB-SEM. TEM images of viable *K. pneumoniae* cells revealed a uniform envelope, continuous around the entire cell (Figure 4A), with the inner and outer plasma membranes enclosing a peptidoglycan layer of approximately 5 nm in thickness (Figure 4B). In contrast, *K. pneumoniae* cells incubated on surface T2 showed indications of envelope indentation in areas contacting one or more nanostructure (Figure 4C – D); furthermore, each nanostructure tip was located within the cell. These observations provide further evidence that contact between nanostructures and bacteria induce cell envelope stretching, leading to rupture of the cell.

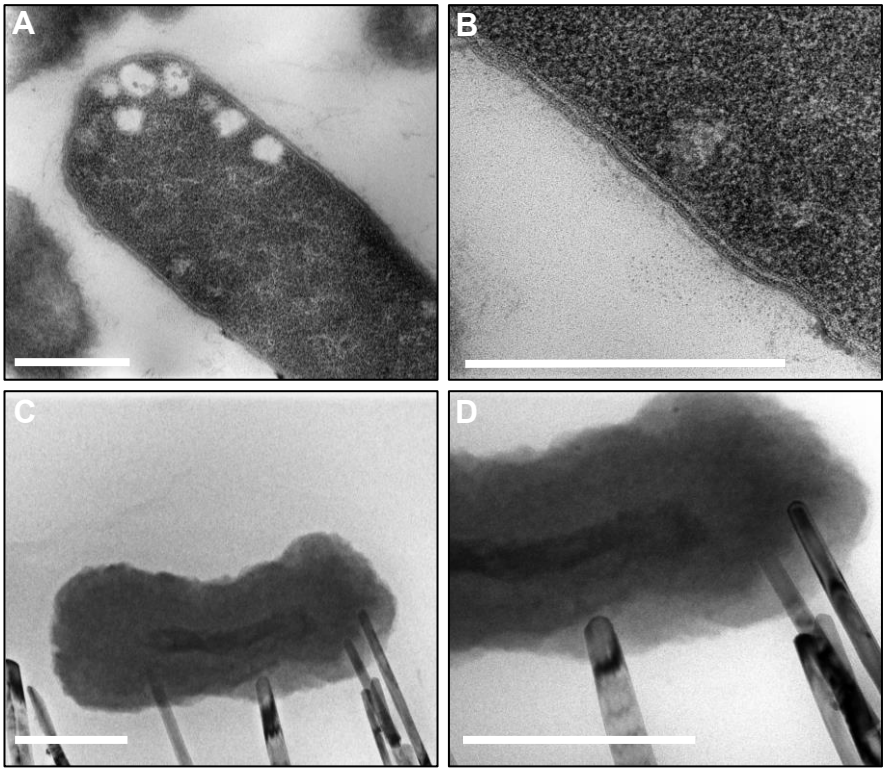

Figure 4. *TEM images of K. pneumoniae. K. pneumoniae is a Gram-negative bacterium with a rod-shaped morphology and a cell envelope that is uniform and continuous around the cell (A). The envelope is comprised of outer and inner plasma membranes separated by a peptidoglycan layer (≈ 5 nm) (B). In contrast, the envelope of K. pneumoniae was not uniform when incubated on surface T2; instead, areas in contact with nanostructures were indented (C). At higher magnification these regions appear stretched (D). Scale bar 500 nm.*

Analysis of bacterial ultrastructure was also attempted using FIB-SEM. A focused beam of gallium ions was used to generate a cross section approximately 250 nm in thickness through three bacterial cells suspected of having structurally-compromised envelopes (Figure 5A - B). The resulting section was lifted from the surface and analysed under TEM. TEM analysis identified multiple nanostructures inside one cell (Figure 5C). These supported observations made under SEM and TEM that nanostructure contact leads to stretching of the bacterial cell envelope and rupture.

The combined image data collected in this study corroborate with current biophysical models, attributing contact killing to mechanical stretching of the cell, resulting in peptidoglycan rupture and cell deformation [13,14]. However, the physical properties that constitute an ideal bactericidal surface remain to be confirmed.

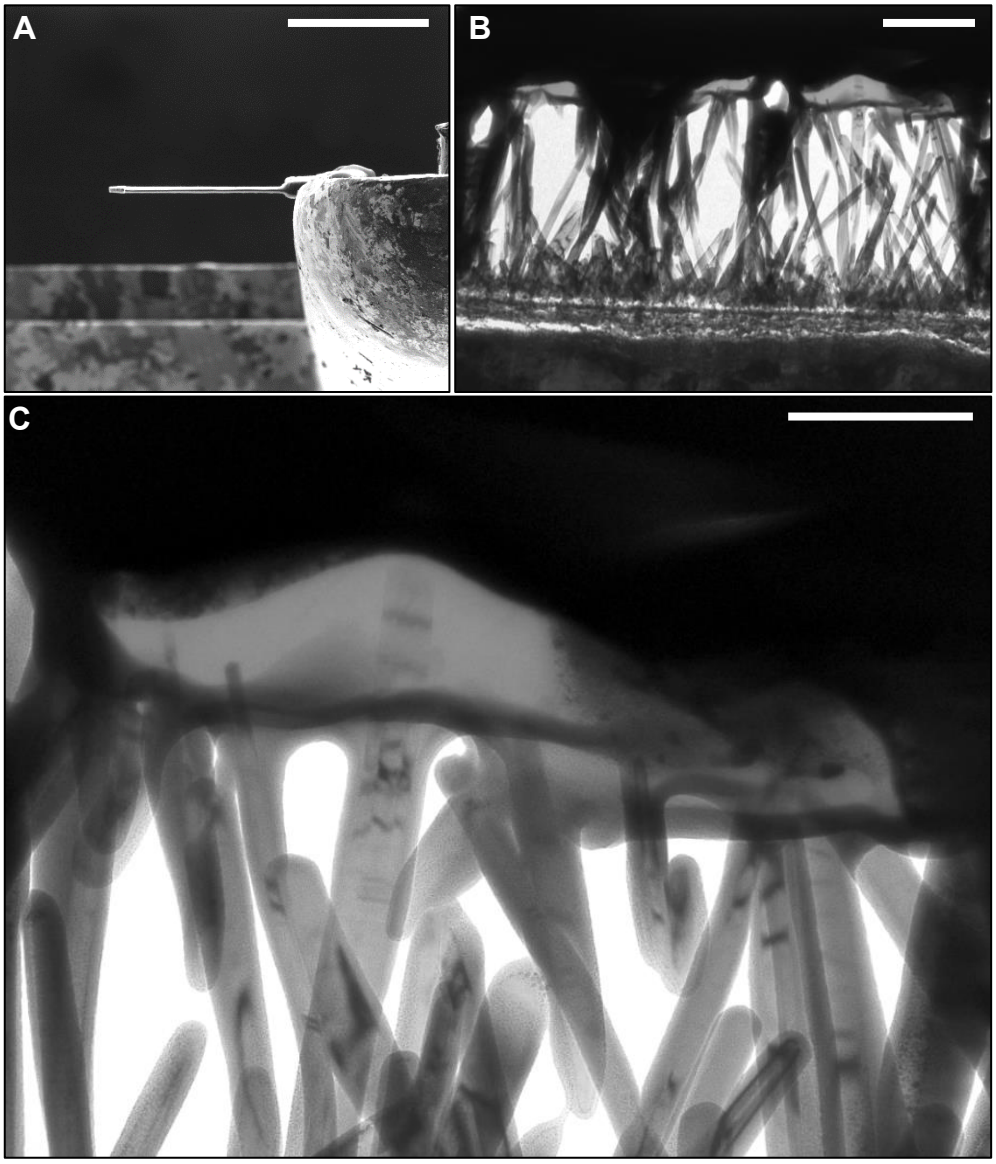

Figure 5. *FIB-SEM analysis of K. pneumoniae on a nanostructured substrate. A 250 nm cross section of three bacterial cells was generated by FIB milling and attached to a lift-out grid (A-B). At higher magnification, TiO_2 nanostructures can be seen inside one bacterium, suggesting the envelope has been penetrated (C). Scale bars (A = 10 µm), (B-C = 500 nm)*

A comparison of EM with alternative imaging techniques

For visualising the interaction between bacterial cells and nanostructures, EM has several advantages over alternate imaging techniques. As shown in this study, EM enables bacterial features, and ultrastructure, to be studied with nanometre resolution (Figure 6A – 6B). This capability is essential for identifying morphological differences in bacteria. However, EM is not without limitation, sample preparation involves multiple steps, including fixation, dehydration, and in TEM, staining. These processes can be protracted, and mean that live cell events cannot be studied.

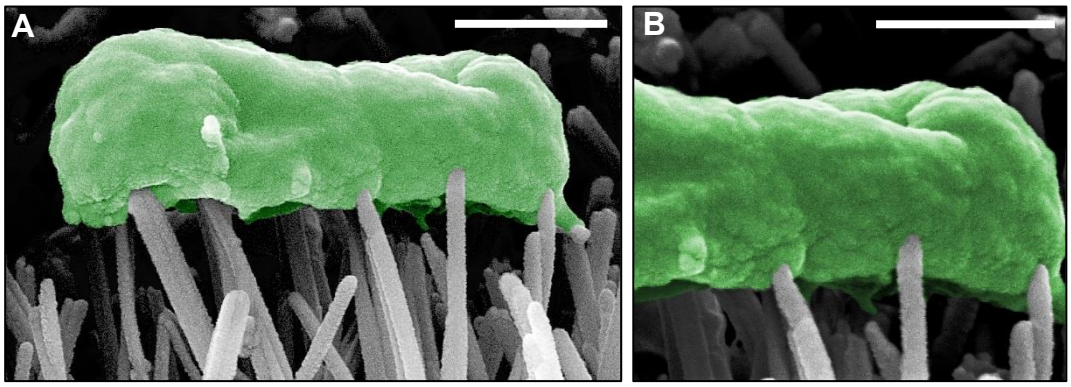

Figure 6. *False colour SEM image of K. pneumoniae suspended between multiple TiO_2 nanostructures (A). A higher magnification image reveals an indentation in the bacterial cell envelope (B). This morphology was not observed on flat titanium surfaces, implying that nanostructures are initiating cell deformation. Scale bar = 500 nm.*

By comparison, fluorescence microscopy can monitor live cell events, however, resolution constraints make it difficult to clearly resolve damage in bacterial membranes which may be induced by nanostructures. To fully understand contact killing, viewing the nanotopography in contact with bacteria is crucial, however, fluorescence microscopy only highlights cells, leaving abiotic surfaces concealed in the background (Figure 7) [15]. These factors limit the potential of using fluorescence microscopy for visualising the interaction between bacteria and nanostructured surfaces.

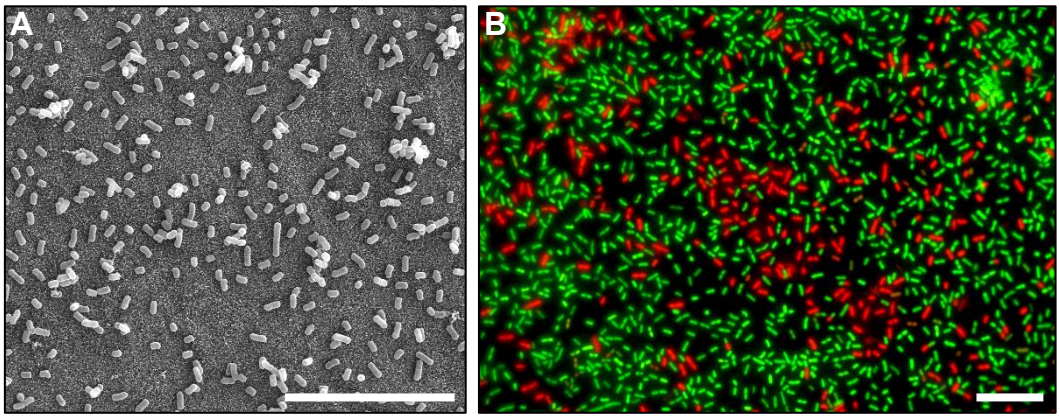

Figure 7. *Images of K. pneumoniae on a nanostructured surface, as seen under SEM (A) and fluorescence microscope [stained with LIVE/DEAD cell viability fluorophores SYTO9 and propidium iodide] (B). Under SEM, nanostructures are visible, whilst under fluorescence microscope, only bacterial cells are highlighted. Scale bars 20 µm.*

Atomic force microscopy (AFM) has also been utilised for imaging bacterial cells on nanostructured surfaces [16,17] . Like EM, AFM can resolve nanoscale features on bacteria whilst also providing mechanical information about the cell, AFM also has the capability to image living specimens in aqueous conditions. However, to acquire AFM images, a tip must interact with a surface through tapping or continuous contact. These operating modes increase the possibility of sample damage and tip-induced perturbations, which may affect data interpretation [18]. Furthermore, achieving high resolution images with AFM often requires longer scanning times when compared to EM, and greater consideration of instrumental set up.

Conclusion

Based on the imaging data presented here, TiO_2 nanostructured surfaces are shown to compromise the cell envelope of Gram-negative bacteria in a contact-dependent manner. Evidence is provided that the nanostructures exert a stretching force across the cell envelope. This process is proposed to cause bacterial cell rupture, leading to loss of turgor pressure and deformation, and ultimately to bacterial cell death.

SEM analysis provided visual evidence of cell envelope stretching and deformation by TiO_2 nanostructures in Gram-negative bacteria *E. coli* and *K. pneumoniae*. In contrast, for *S. aureus* there were no indications of structural deformation on any surface type. These differential effects were most likely related to differences in cell envelope structure between Gram-positive and Gram-negative bacteria.

This was further supported by TEM analysis of *K. pneumoniae,* which revealed structural deformation in the form of envelope stretching. Critically, these effects were only seen for bacteria in contact with T2 substrate. Analysis of a FIB lift-out from this substrate highlighted multiple piercing events in a single cell, corroborating with SEM and TEM analysis. Future studies will develop TEM and FIB-SEM imaging techniques to more clearly resolve the mechanistic effects of nanostructures on the bacterial cell envelope. This will enable the antimicrobial potential of nanostructured surfaces to be maximised.

References

1. Von Eiff, C., Jansen, B., Kohnen, W. & Becker, K. Infections associated with medical devices: Pathogenesis, management and prophylaxis. *Drugs* **65,** 179–214 (2005).

2. Darouiche, R. O. Treatment of infections associated with surgical implants. *N Engl J Med* **350,** 1422–1429 (2004).

3. Francolini, I. & Donelli, G. Prevention and control of biofilm-based medical-device-related infections. *FEMS Immunol. Med. Microbiol.* **59,** 227–238 (2010).

4. Bryers, J. D. Medical biofilms. *Biotechnol. Bioeng.* **100,** 1–18 (2008).

5. Campoccia, D., Montanaro, L. & Arciola, C. R. The significance of infection related to orthopedic devices and issues of antibiotic resistance. *Biomaterials* **27,** 2331–2339 (2006).

6. Briggs, T. W. Getting it right first time: improving the quality of orthopaedic care within the national health service in England. 1–32 (2011).

7. Busscher, H. J. *et al.* Biomaterial-associated infection: locating the finish line in the race for the surface. *Sci. Transl. Med.* **4,** 1–11 (2012).

8. Tripathy, A., Sen, P., Su, B. & Briscoe, W. H. Natural and bioinspired nanostructured bactericidal surfaces. *Adv. Colloid Interface Sci.* **248,** 85–104 (2017).

9. Ivanova, E. P. *et al.* Natural bactericidal surfaces: mechanical rupture of *Pseudomondas aeruginosa* cells by cicada wings. *Small* **8,** 2489–2494 (2012).

10. Ivanova, E. P. *et al.* Bactericidal activity of black silicon. *Nat. Commun.* **4,** 1 – 7 (2013).

11. Diu, T. *et al.* Cicada-inspired cell-instructive nanopatterned arrays. *Sci. Rep.* **4,** 1 – 7 (2014).

12. Hasan, J. *et al.* Selective bactericidal activity of nanopatterned superhydrophobic cicada Psaltoda claripennis wing surfaces. *Appl. Microbiol. Biotechnol.* **97,** 9257–9262 (2013).

13. Pogodin, S. *et al.* Biophysical model of bacterial cell interactions with nanopatterned cicada wing surfaces. *Biophys. J.* **104,** 835–840 (2013).

14. Li, X. & Chen, T. Enhancement and suppression effects of a nanopatterned surface on bacterial adhesion. *Phys. Rev. E* **93,** 1–7 (2016).

15. Lichtman, J. W. & Conchello, J. A. Fluorescence microscopy. *Nat. Methods* **2,** 910–919 (2005).

16. Bandara, C. D. *et al.* Bactericidal effects of natural nanotopography of dragonfly wing on Escherichia coli. *ACS Appl. Mater. Interfaces* **9,** 6746–6760 (2017).

17. Kelleher, S. M. *et al.* Cicada wing surface topography: an investigation into the bactericidal properties of nanostructural features. *ACS Appl. Mater. Interfaces* **8,** 14966–14974 (2016).

18. Lal, R. & John, S. A. Biological applications of atomic force microscopy. *Am. Physiol. Soc.* **266,** 1–21 (1994).

Biography

Joshua Jenkins is a postgraduate researcher at the University of Bristol, currently studying for a PhD in Applied Clinical Material Science. He received his BSc in Cellular and Molecular Medicine from the University of Bristol. His current research involves studying physical mechanisms to prevent bacterial biofilm formation on clinical materials.

Acknowledgements

The authors would like to acknowledge Judith Mantell and Chris Neil for assistance with SEM and TEM studies carried out in the Wolfson Bioimaging Facility at The University of Bristol, and Ian Griffiths for assistance with FIB-SEM, carried out in the Interface Analysis Centre at The University of Bristol. EDX analysis was performed in the Chemistry Imaging Facility at The University of Bristol. The authors would like to acknowledge Medical Research Council (MRC) funding.

Corresponding Author details

Joshua Jenkins
Bristol Dental School, University of Bristol, Bristol, BS1 2LY
Email: Joshua.Jenkins@bristol.ac.uk